Makris, N., Gazetas, G. & Delis, E. (1996). *Géotechnique* **46**, No. 1, 33–50

Dynamic soil–pile–foundation–structure interaction: records and predictions

N. MAKRIS,* G. GAZETAS† and E. DELIS‡

The problem of soil–pile–foundation–superstructure interaction is examined, and a simple rational procedure to analyse the response of a structure supported on pile groups is presented. This procedure combines theories for the computation of the dynamic impedances and kinematic–seismic response factors of pile foundations with a multi-degree-of-freedom structural model. The procedure is applied to compute the response of a bridge in Rio Dell, California, which was shaken by the $M_s = 7{\cdot}0$ Petrolia earthquake in 1992. The predicted response agrees well with recorded data. The significance of considering the frequency-dependence of the pile foundation impedances in the analysis of the response of the superstructure is discussed.

KEYWORDS: case history; dynamics; earthquakes; embankments; piles; soil–structure interaction.

L'article s'intéresse aux problèmes générés par les interactions sol–pieu fondation–superstructure et présente une procédure rationelle simple permettant d'analyser la réponse d'une structure fondée sur groupes de pieux. Cette procédure combine les théories disponibles, permettant le calcul des impédances dynamiques et des facteurs de réponse sismique d'une fondation sur pieux, à un modèle structural à n degrés de liberté. La procédure a été appliquée à un pont du Rio Dell, en Californie, qui a été soumis en 1992 au séisme de Pétrolia de $M_s = 7{\cdot}0$. La réporte prévue correspond bien aux raleun observées. L'article montre également qu'il est importance de considèrer, lors de l'analyse de la réponse de la superstructure, que la fréquence est fonction de l'impedance des pieux.

INTRODUCTION

When a flexible structure is supported by a stiff foundation, it is natural to assume that the input motion from a potential earthquake at the foundation level of the structure is merely that of the free field. However, as the ratio of the stiffness of the structure to that of the foundation increases, the superstructure's response interacts through its foundation and the surrounding soil creates additional soil deformations, so that the motion in the vicinity of the foundation can differ substantially from that of the free field. This Paper presents a simplified yet realistic method of analysis for the case where the foundation of the superstructure consists of pile groups.

Assuming linear soil–foundation–superstructure response, the system analysis under seismic excitation can be performed in three consecutive steps as shown in Fig. 1: first find out the motion of the foundation in the absence of the superstructure (the so-called foundation input motion), which includes translational as well as rotational components; then determine the dynamic impedances (springs and dashpots) associated with swaying, vertical, rocking and cross-swaying–rocking oscillations of the foundation; and lastly calculate the seismic response of the superstructure supported on the springs and dashpots and subjected at the ground base to the foundation input motion. For the first two steps, several formulations have been developed for pile foundations and have been reviewed by Novak (1991) and Pender (1993).

Despite remarkable advances over the past two decades in pile foundation dynamics, little is known about the significance of pile foundation–superstructure interaction, even for important structures such as like bridges. For instance, in several cases the assumption that the pile group is a fixed monolithic support prevails. In fact, more often the foundation compliance is represented by a single real-valued spring. Plausible reasons for the lack of established procedures for the analysis of structures supported on pile foundations include the following.

Manuscript received 22 February 1994; accepted 7 September 1994.
Discussion on this Paper closes 3 June 1996; for further details see p. ii.
* Department of Civil Engineering and Geological Sciences, University of Notre Dame, Indiana.
† Department of Civil Engineering, National Technical University, Athens.
‡ California Department of Transportation.

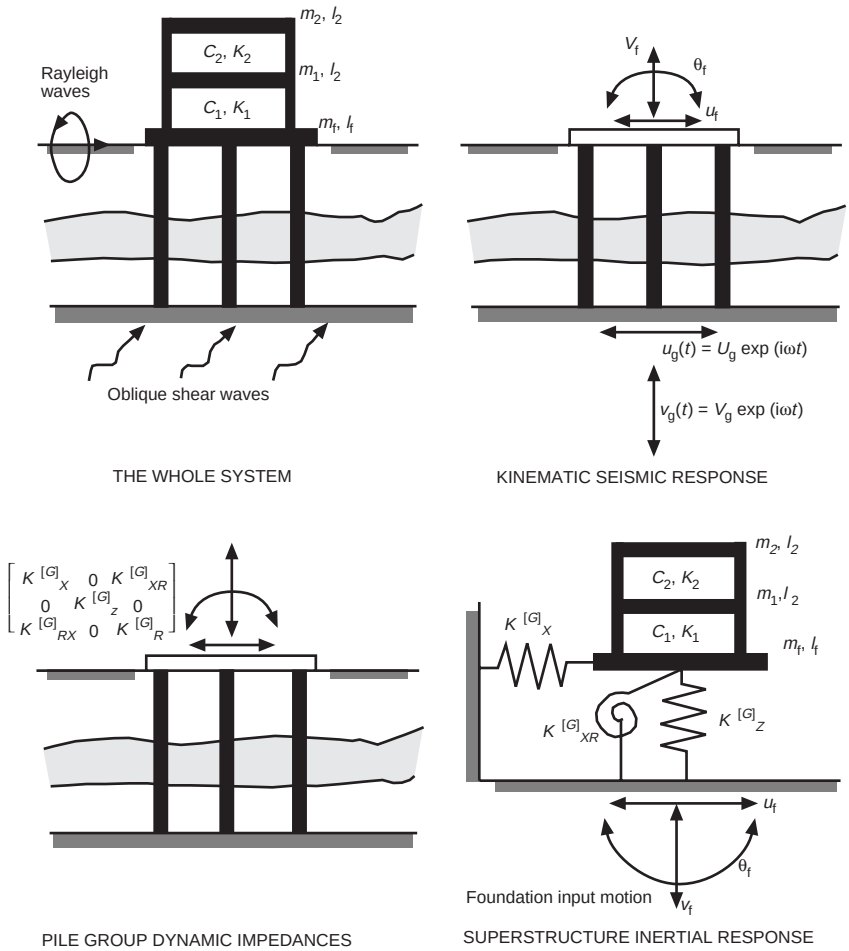

Fig. 1. General procedure for seismic soil–pile foundation–superstructure interaction

(*a*) Most of the research results published on the dynamic response of pile foundations is scattered and presented in such a form that is of little use to the bridge (structural) engineer.
(*b*) Some of the most reliable methods for analysing the response of pile foundations rely on proprietary computer codes.

The procedure for seismic soil–pile foundation–superstructure interaction described in this paper makes use of physical motivated approximations. Existing theories and solutions are used to compute of the dynamic impedances and kinematic seismic response factors of pile foundations. The superstructure is idealized with a multi-degree-of-freedom model supported by realistic frequency-dependent springs and dashpots. Using this simple procedure the significance of considering the frequency dependence of pile foundation impedances to the response of the superstructure can be investigated easily. The methodology is validated by a prediction of the response of Painter Street Bridge in Rio Dell, California, which has been instrumented since 1977 by the California Division of Mines and Geology and survived in 1992 Petrolia earthquake. The predicted response using the proposed procedure agrees well with recorded data, and considerable supporting evidence on the significance of the soil–pile foundation–superstructure interaction is given.

PROPOSED APPROXIMATE PROCEDURE

Novak (1991) presents a variety of methods of solution for the seismic soil–pile–foundation response analysis. In this paper simple, yet realistic, solutions involved in each step are outlined. The methods used are physically motivated and computationally convenient; extensive comparative studies have also shown their basic validity.

Foundation input motion

The input motion to the structural system is induced at the foundation. In general, the support motion induced to the foundation is different from that of the free-field seismic motion. This difference is due to the scattered wave field generated from the difference between pile and soil rigidities. Nevertheless, for motions that are not rich in high frequencies, the scattered field is weak, and the support motion can be considered to be approximately equal to that of the free field (Fan *et al.*, 1991; Gazetas, 1984; Kaynia & Novak, 1992; Makris & Gazetas, 1992; Mamoon & Banerjee, 1990; Tajimi, 1977). For instance, for Painter Street Bridge studied in the sequel, the soil deposit has an average shear velocity V_s of about 200 m/s (Heuze & Swift, 1991); the pile diameter d is 0·36 m. Accordingly, even for the high frequency content of the input motion ($f \approx 10$ Hz, see Fig. 6), the dimensionless frequency $a_0 = 2\pi fd/V_s$ is of the order of only 0·1. From studies on vertically propagating shear waves in homogeneous soil deposits (Fan *et al.*, 1991), the kinematic–seismic response factors (head-group displacement over free-field displacement) are very close to unity, even at values of the dimensionless frequency $a_0 > 0{\cdot}1$.

Waves other than vertical S-waves also participate in ground-shaking. Seismic–kinematic response factors for SV waves, P waves and Rayleigh surface waves are given by Mamoon & Banerjee (1990) Kaynia & Novak (1992), Makris (1994) and Makris & Badoni (1995). For all these types of wave which produce a vertical component of the seismic input motion, the kinematic response factors are also close to unity. Only in some cases do SV waves with a high angle of incidence result in kinematic response factors of the order of 0·90. Based on such supporting analytical evidence, in most cases the excitation input motion at the level of the pile foundation can be assumed to be equal to that of the free-field motion. Only at very high frequencies or for very soft soils will a reduction be needed. Moreover, in the case of Rayleigh waves and SV waves, a pile group produces an effective rocking input motion, whereas for oblique incidence SH waves the foundation experiences torsional excitation. These motions are the result of phase differences that the seismic input has at the locations of different piles in the group (wave passage effect); their intensity depends on the frequency content of the seismic input and the geometry of the pile group.

Dynamic impedances of pile foundation

The dynamic stiffness of a pile group, in any vibration mode, can be calculated using the dynamic stiffness of single pile in conjunction with dynamic interaction factors. This method, originally introduced for static loads by Poulos (1968), and later validated for dynamic loads by Kaynia & Kausel (1982), Sanchez-Salinero (1983) and Roesset (1984), can be used with confidence—at least for groups of fewer than 50 piles. Dynamic interaction factors for various modes of loading are available in the form of non-dimensional graphs (Gazetas, Fan, Kaynia & Kausel, 1991) and, in some cases, closed-form expressions derived from a beam on a Winkler foundation model in conjunction with simplified wave propagation theory (Makris & Gazetas, 1992). For example, the horizontal dynamic interaction factor for two fixed-head long piles in a homogeneous stratum takes the form

$$\alpha_X(S, \theta) = \tfrac{3}{4}\psi(S, \theta) \times \frac{k_X(\omega) + \mathrm{i}\omega c_X(\omega)}{k_X(\omega) + \mathrm{i}\omega c_X(\omega) - m\omega^2} \tag{1}$$

where k_X and c_X are distributed spring and dashpot coefficients and $\psi(r, \theta)$ is an approximate attenuation function proposed by (Makris & Gazetas, 1992)

$$\psi(S, \theta) = \psi(S, 0)(\cos\theta)^2 + \psi\left(S, \frac{\pi}{2}\right)(\sin\theta)^2 \tag{2}$$

$$\psi(S, 0) = \left(\frac{d}{2S}\right)^{1/2} \times \exp\left[-(\beta_s + \mathrm{i})\frac{\omega(S - d/2)}{V_{La}}\right] \tag{3}$$

$$\psi\left(S, \frac{\pi}{2}\right) = \left(\frac{d}{2S}\right)^{1/2} \times \exp\left[-(\beta_s + \mathrm{i})\frac{\omega(S - d/2)}{V_s}\right] \tag{4}$$

where i is $\sqrt{-1}$, S is the distance between the axes of two piles and θ is the angle between the direction of loading and the line connecting the axes of the two piles. β_s is hysteretic damping in the soil, V_s is the shear wave velocity of the soil, and V_{La}—an apparent velocity of the compression–extension waves, given the name Lysmer's analog velocity—is $V_{La} = 3{\cdot}4V_s/\pi(1 - \nu)$ (Gazetas & Dobry, 1984a, 1984b).

For vertical and rocking modes, pile motion is along the axial direction, and the interaction factors for two floating piles in a homogeneous half-space is

$$\alpha_Z(S) = \left(\frac{d}{2S}\right)^{1/2} \exp\left[-(\beta_s + \mathrm{i})\frac{\omega(S - d/2)}{V_s}\right] \tag{5}$$

When the dynamic stiffnesses of the single pile and dynamic interaction factors between any two piles are known, the dynamic stiffnesses of a group of piles using superposition can be calculated (Makris, Cordosa, Badoni & Delis, 1993). Accordingly, the horizontal dynamic stiffness of a pile group consisting of N piles is simply

$$\mathscr{K}_X^{[G]} = \mathscr{K}_X^{[1]} \sum_{i=1}^{N} \sum_{j=1}^{N} \varepsilon_{X(i,j)} \tag{6}$$

where the $\varepsilon_{X(i,j)}$ is the inverse of the matrix $\alpha_{X(i,j)}$ obtained from equation (1).

The vertical dynamic stiffness of the group is also given by an equivalent expression

$$\mathscr{K}_Z^{[G]} = \mathscr{K}_Z^{[1]} \sum_{i=1}^{N} \sum_{j=1}^{N} \varepsilon_{Z(i,j)} \tag{7}$$

where $\varepsilon_{Z(i,j)}$ is the inverse of the matrix $\alpha_{Z(i,j)}$ obtained from equation (5).

The rocking group-dynamic stiffness can be derived using a similar analysis (Dobry & Gazetas, 1988; Makris *et al.*, 1993) as

$$\mathscr{K}_R^{[G]} = \mathscr{K}_Z^{[1]} \sum_{i=1}^{N} x_i \sum_{j=1}^{N} x_j \varepsilon_{Z(i,j)} \tag{8}$$

where x_i is the distance of pile i from the axis about which rotation occurs.

For the cross-horizontal–rocking interaction factors it has been found (Gazetas *et al.*, 1991) that the approximation

$$\alpha_{XR(i,j)} \approx \alpha^2_{X(i,j)} \tag{9}$$

proposed by Randolph (1977) for static loaded piles, is also valid under dynamic loading. Accordingly, the cross-horizontal–rocking group stiffness is

$$\mathscr{K}_{XR}^{[G]} = \mathscr{K}_{XR}^{[1]} \sum_{i=1}^{N} \sum_{j=1}^{N} \varepsilon_{XR(i,j)} \tag{10}$$

where $\varepsilon_{XR(i,j)}$ is the element of the inverse of matrix $\alpha_{XR(i,j)}$ given by equation (9).

The dynamic stiffness of the single pile is usually expressed in the form

$$\mathscr{K}_\alpha^{[1]} = K_\alpha^{[1]} \{k_{\alpha 1}^{[1]}(\omega) + i k_{\alpha 2}^{[1]}(\omega)\} \tag{11}$$

where the index α denotes the degree of freedom (X, Z, R, RX) and the quantity within brackets is the associated dynamic stiffness coefficient. It can be obtained from published solutions in the form of formulae and charts using Novak's plane–strain formulation (Novak, 1974; Novak & Aboul-Ella, 1978), using finite element analysis (Blaney, Kausel & Roesset, 1976; Kuhlemeyer, 1979; Roesset, 1984), boundary element analysis (Kaynia & Kausel, 1982; Banerjee & Sen, 1987; Kaynia & Novak, 1992),

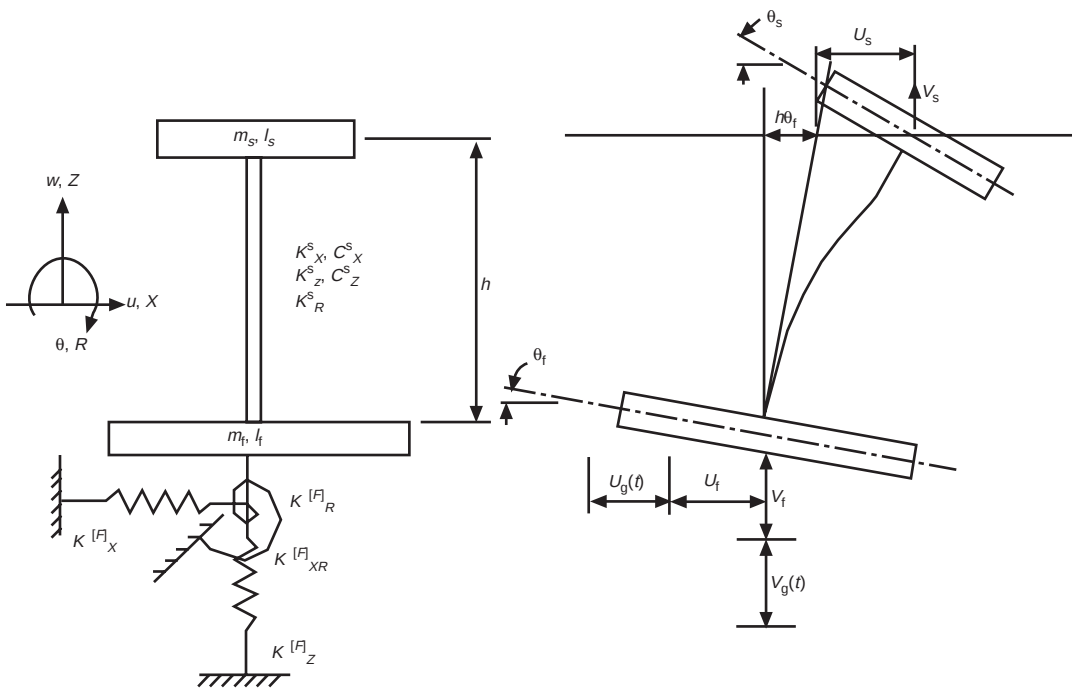

Fig. 2. Pile foundation–superstructure idealization

Fig. 3. Painter Street Bridge after earthquake on 25 April 1992: (above) over highway 101; (right) north pier

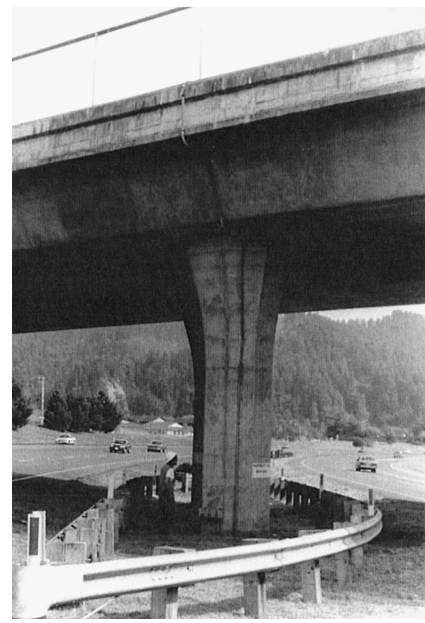

and from beam on Winkler foundation formulations (Makris & Gazetas, 1993; Kavvadas & Gazetas, 1993).

Determination of system seismic response

The foundation–superstructure system is idealized with the six degrees of freedom system shown in Fig. 2. Such simple idealization is realistic for the study of bridge response. In Fig. 2 m_s, m_f, I_s and I_f are the masses and moments of inertia of the superstructure and the foundation. For a multi-span bridge, m_s and I_s are the mass and moment of inertia of the deck corresponding to one span plus a, usually small, contribution from the bridge pier. K_X^s, K_Z^s *and* K_R^s are the horizontal, vertical and rotational stiffnesses of the superstructure. For the section of the superstructure considered, K_X^s, K_Z^s and K_R^s are the combinations of the stiffnesses of the bridge pier and the bridge deck. This is a reasonable approximation when the abutments of the bridge and the foundation of the bridge pier experience the same input motion. For relatively short bridges this approximation can be realistic in some cases. However, for relatively long bridges, the abutment and pier base motions are likely to be different and a more sophisticated model might be more appropriate. Nevertheless, for bridges with very long spans the contribution from the deck stiffness might be negligible and the model becomes again realistic, as the entire horizontal stiffness of the superstructure comes essentially from the bridge pier. C_X^s and C_Z^s are constants of the superstructure damping, which is assumed to be of linear viscous nature. $\mathscr{K}_X^{[F]}$, $\mathscr{K}_Z^{[F]}$, $\mathscr{K}_R^{[F]}$ and $\mathscr{K}_{RX}^{[F]}$ are the horizontal, vertical, rocking and cross-horizontal–rocking impedances of the pile foundation and are complex valued quantities.

The degrees of freedom of the structural model depicted in Fig. 2 are: $\langle u_s,\ v_s,\ h\theta_s,\ u_f,\ v_f,\ h\theta_f\rangle$. With the linear range and for small rotations, the equations of motion of the system subjected to a ground acceleration are transformed in the frequency domain and expressed in matrix form as

$$[S(\omega)]\{U(\omega)\} = \{F(\omega)\} \tag{12}$$

in which $\{U(\omega)\}$ is the Fourier transform of the response vector $\langle u_s,\ v_s,\ h\theta_s,\ u_f,\ v_f,\ h\theta_f\rangle$ and $\{F(\omega)\}$ is the Fourier transform of the excitation vector $\langle -\ddot{u}_g,\ -\ddot{v}_g,\ 0,\ -(1+\mu)\ddot{u}_g,\ -(1+\mu)\ddot{v}_g,\ -\ddot{u}_g\rangle$, with $\mu = m_f/m_s$. The elements of the matrix $[S]$ are given in Appendix 1. The Fourier transform of the reactions from the pile foundation are given by

$$\mathscr{F}\{P_X^{[F]}(t)\} = \mathscr{K}_X^{[F]}(\omega)u_f(\omega) + \mathscr{K}_{XR}^{[F]}(\omega)\theta_f(\omega) \tag{13}$$

$$\mathscr{F}\{P_Z^{[F]}(t)\} = \mathscr{K}_Z^{[F]}(\omega)v_f(\omega) \tag{14}$$

$$\mathscr{F}\{M_R^{[F]}(t)\} = \mathscr{K}_{RX}^{[F]}(\theta)u_f(\omega) + \mathscr{K}_R^{[F]}(\omega)\theta_f(\omega) \tag{15}$$

where $\mathscr{K}_X^{[F]}$, $\mathscr{K}_Z^{[F]}$, $\mathscr{K}_R^{[F]}$ and $\mathscr{K}_{RX}^{[F]} = \mathscr{K}_{XR}^{[F]}$ are the horizontal, vertical, rocking and cross-horizontal–rocking impedances of the pile foundation, and can be written in the form given in equation (11) with superscript [1] replaced by $[F]$.

The remaining parameters appearing in the dynamic stiffness matrix $[S]$ are

$$\Omega_{Xs} = \left(\frac{K_X^s}{m_s}\right)^{1/2}, \quad \Omega_{Zs} = \left(\frac{K_Z^s}{m_s}\right)^{1/2},$$

$$\Omega_{Rs} = \left(\frac{K_R^s}{m_s h^2}\right)^{1/2}, \quad \Omega_{XRs} = \left(\frac{K_{xR}^s}{m_s h}\right)^{1/2} \tag{16}$$

$$\xi_{Xs} = \frac{C_X^s}{2m_2\Omega_{Xs}}, \quad \xi_{Zs} = \frac{C_Z^s}{2m_s\Omega_{Zs}} \tag{17}$$

$$\Omega_{Xf} = \left(\frac{K_X^{[F]}}{m_s}\right)^{1/2}, \quad \Omega_{Zf} = \left(\frac{K_Z^{[F]}}{m_s}\right)^{1/2},$$

$$\Omega_{Rf} = \left(\frac{K_R^{[F]}}{m_s h^2}\right), \quad \Omega_{XRf} = \left(\frac{K_{XR}^{[F]}}{m_s h}\right)^{1/2} \tag{18}$$

$$\rho_s = \left(\frac{I_s}{m_s}\right)^{1/2}, \quad \rho_f = \left(\frac{I_f}{m_f}\right)^{1/2} \tag{19}$$

The system response in the time domain is obtained by the inverse Fourier transform of the response vector $\{U(\omega)\}$ (Clough & Penzien, 1993)

$$\{U(t)\} = \frac{1}{2\pi}\int_{-\infty}^{\infty}[H(\omega)]\{F(\theta)\}\exp(i\omega t)\,d\omega \tag{20}$$

where $[H(\omega)]$ is the inverse of the matrix $[S(\theta)]$. Relative velocities and acceleration responses are obtained from equation (20) after the matrix $[H(\theta)]$ has been premultiplied by $i\omega$ and $-\omega^2$, respectively. Numerical solutions are then derived by the discrete Fourier transform method (Veletsos & Ventura, 1985).

The procedure presented is not restricted to the simple structural model already used. Additional degrees of freedom for the structure could be incorporated to account for the motion of end abutments and the torsional vibration of the bridge about the vertical axis. Here the simple structural model is introduced to present and validate an integrated procedure for the analysis of soil–pile group–superstructure interaction. Despite its simplicity, the model predicts well the recorded motion of Painter Street Bridge in the 1992 Petrolia earthquake.

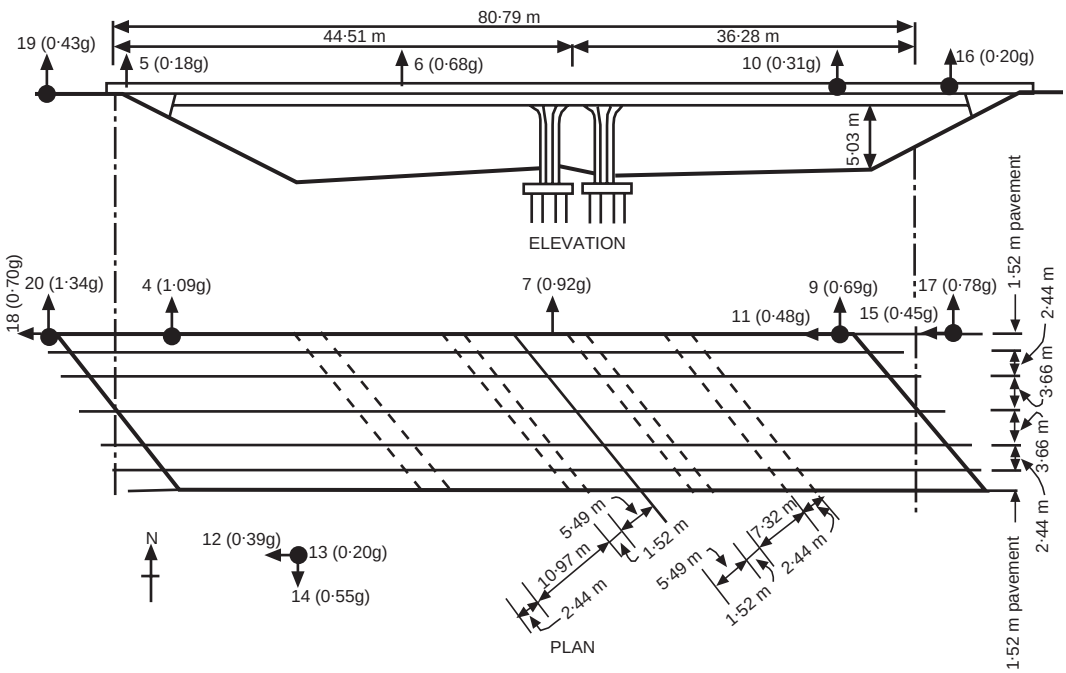

Fig. 4. Elevation and plan view of Painter Street Bridge (values in parentheses indicate peak recorded acceleration)

Table 1. Earthquake records on Painter Street Bridge (from Maroney *et al.*, 1990)

Earthquake	Date	Magnitude M_L	Epicentral distance: km	Peak acceleration: g					
				C12	C13	C14	C6	C7	C8
Trinidad	8 November 1980	6·9	72	0·15	0·03	0·06	0·34	—	0·25
Rio Dell	16 December 1982	4·4	15	—	—	—	0·39	0·43	0·59
Cape Mendocino	24 August 1983	5·5	61	—	—	—	0·27	0·22	0·16
Event 1	21 November 1986	5·1	32	0·46	0·08	0·16	0·24	0·26	0·33
Event 2	21 November 1986	5·1	26	0·15	0·02	0·12	0·21	0·36	0·29
Cape Mendocino	31 July 1987	5·5	28	0·15	0·04	0·09	—	0·34	0·27

APPLICATION TO PAINTER STREET BRIDGE

Background

Painter Street Bridge, near Rio Dell in northern California, is a continuous, two-span, cast in place, prestressed post-tensioned concrete, box girder bridge. It is typical of concrete bridges constructed in 1973 and spans a four-lane highway. The structure has one span of 146 ft* and one of 119 ft. It is 52 ft wide. The two end abutments and the two-column bent are skewed at 39°. The columns are approximately 20 ft high. The bent is supported by two pile groups, each consisting of 20 (4×5) driven concrete friction piles. Fig. 3 shows Painter Street Bridge over highway 101 and the north pier of the bridge. An elevation and plan view of the bridge, together with the location of the accelerometers and the recorded peak accerations, are given in Fig. 4. The cross-section of the bridge and a plan view of the pile group are shown in Fig. 5.

Painter Street Bridge was instrumented in 1977 by the California Division of Mines and Geology. Several earthquakes from 1980 to 1987 ranging in magnitude from $4{\cdot}4M_L$ to $6{\cdot}9M_L$ have produced significant accelerograms, the peak values of which are summarized in Table 1. The largest peak acceleration of 0·59 g was near the centre of the bridge deck during a small ($M_L = 4{\cdot}4$) nearby earthquake.

Maroney, Romstad & Chajes (1990) used these records in conjunction with a number of finite element and lumped parameter (stick) models of the entire bridge. However, none of these models accounted for soil–foundation–superstructure interaction. At each abutment, soil–wall interaction was modelled using a single real-valued transverse spring, the stiffness of which was back-calculated from the interpreted small-amplitude fundamental natural period, $T \approx 0{\cdot}30$ s, in lateral vibration.

On 25 April 1992, the bridge was shaken severely by the Petrolia earthquake (of magnitude $M_L = 7{\cdot}1$ and 18 km from the fault). Motions were recorded in all accelerographs, including the one in the free field (channels 12–14), that on the ground

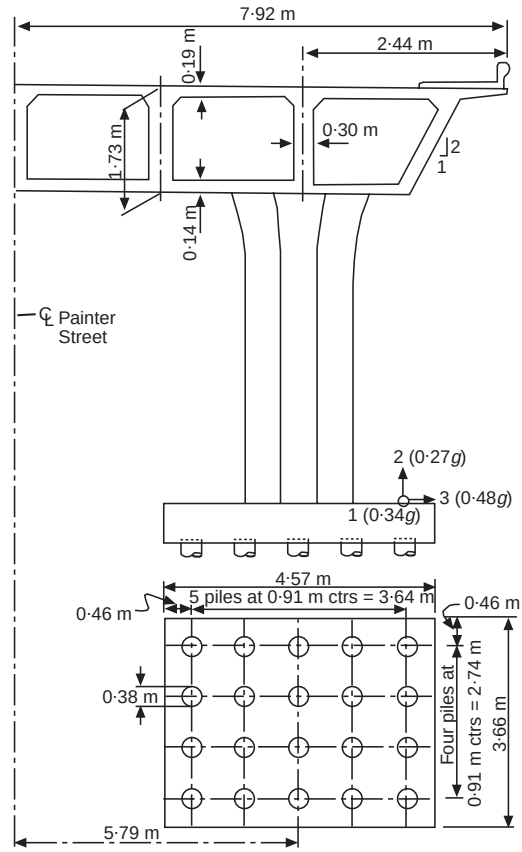

Fig. 5. Cross-section of Painter Street Bridge and plan view of pile group (values in parentheses indicate peak recorded acceleration)

near the east abutment (channels 15–17), that on the deck near the east abutment (channels 9–11), that on top of the footing of one pier (channels 1–3), that on the ground near the west abutment (channels 18–20), that on the deck near the west abutment (channels 4 and 5), and that at the underside of the bridge girder directly above the pier (channel 7). The locations of the accelerographs are shown in Fig. 4, together with the peak recorded acceleration (PRA) for each channel. Of

* 1 ft = 0·3048 m.

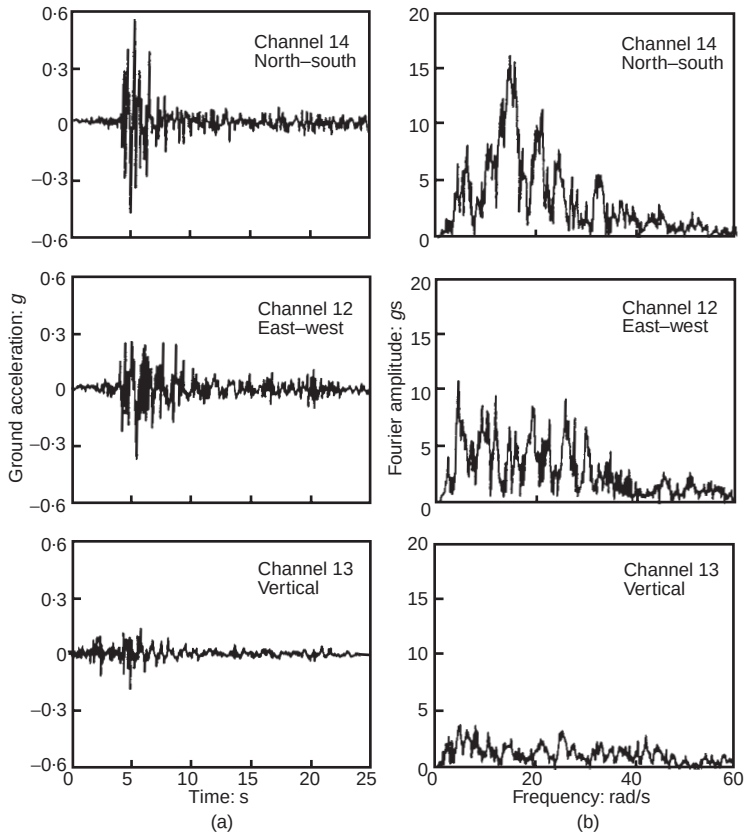

Fig. 6. Free-field acceleration time histories and Fourier amplitude spectra of the Petrolia earthquake, 25 April 1992

particular interest in this Paper are the records of channels 3 (PRA = 0·48 *g*) and 7 (PRA = 0·92 *g*). Despite the very high levels of acceleration, the bridge suffered only minor damage (see Fig. 3). The north–south (channel 14), east–west (channel 12) and vertical (channel 13) free-field records of the Petrolia earthquake are shown in Fig. 6 together with their Fourier amplitudes.

Figure 7 shows the recorded acceleration histories near the east abutment on the ground and on the deck. The horizontal motions recorded on the deck do not differ much from the horizontal motions recorded on the embankment. However, the vertical accelerations recorded on the deck are 40% greater than those for the embankment nearby.

Figure 8 shows the recorded acceleration histories and Fourier amplitude spectra on the ground (embankment) near the west abutment. The time histories in Fig. 8 (channels 18–20) are 100% greater than those in the free-field record (channels 12–14) shown in Fig. 6. This observation indicates that embankments can amplify the input motion considerably; the end abutments can therefore be subjected to an input motion which is stronger than that at the foundation of the centre pier. Fig. 9 shows the recorded acceleration histories and Fourier spectra recorded on the deck near the west abutment. Similar trends are observed.

The response of Painter Street Bridge to the Petrolia earthquake was studied by Sweet (1993), who developed a finite element model of the whole bridge and a large volume of surrounding and supporting soil. Inelastic soil behaviour was modelled using an incremental plasticity model. However, all this sophistication was inconsistent with the modelling of the behaviour of the pile group. Indeed, such modelling was based on the assumption that no pile–soil–pile interaction occurs at 3 ft spacing; the behaviour of the 20 pile group was merely assumed to be 20 times that of a single pile. In fact, pile to pile interaction is expected to play a substantial role in pile group response, given the very close relative spacing of the piles ($S/d \approx 2{\cdot}60$).

The philosophy behind the model developed in

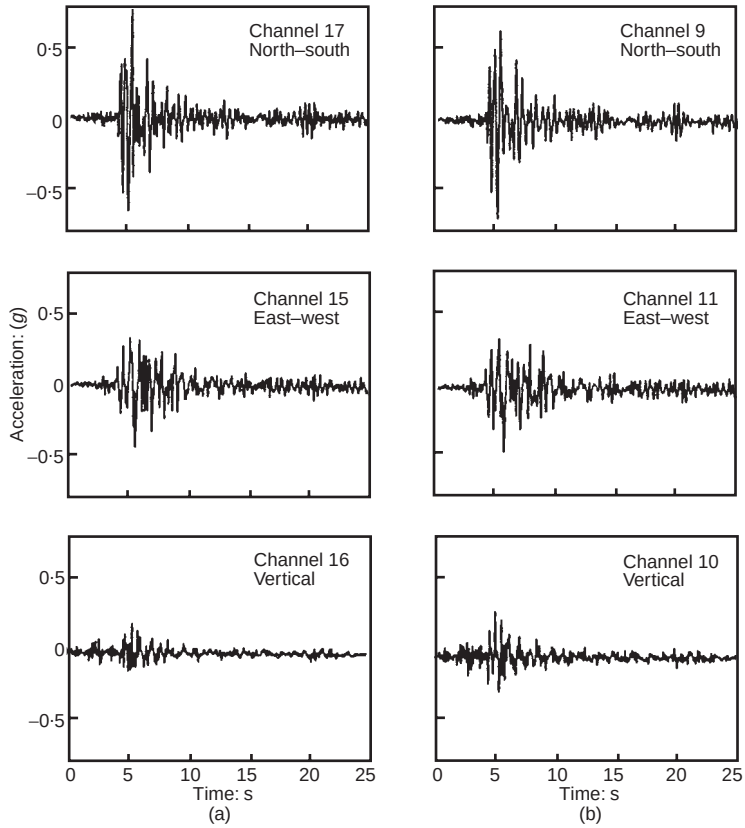

Fig. 7. Recorded time histories near the east abutment; (a) on the ground; (b) on the deck

this Paper is diametrically opposite to that of Sweet (1993). The simplest possible model of the pier deck system is studied, and the pile group foundation is represented by a set of springs and dashpots. However, the frequency-dependent values of these springs and dashpots are calculated in a rational, physically motivated manner, and full account of pile to pile interaction is taken.

Superstructure parameters

Even for a simplified model like the one presented, several uncertainties arise in the determination of its parameters. Such uncertainties relate to the structural stiffness, structural damping, mass distribution, foundation stiffness and pier foundation–soil interaction. Attempts to model the response of the bridge have been given by Maroney *et al.* (1990), who modelled the superstructure in detail, but nevertheless assumed that the foundation stiffness was infinite and the foundation damping was zero.

The model presented here is a simplification of the stick model presented by Maroney *et al.* (1990), who did not consider the longitudinal and torsional modes of the model. The first transverse period of the superstructure was determined by iteration and reported to be 0·28 s during the seismic events of 1982–87 which had produced less intense shaking of the bridge than the Petrolia earthquake (see Table 1). Accordingly, $\Omega_{Xs} = 2\pi/0{\cdot}28\ \text{s} = 22{\cdot}4$ rad/s. The calibrated (back-calculated) horizontal stiffness of the superstructure is reported to be (Maroney *et al.*, 1990) $K_X^s = 39\,000$ kips/ft ($5{\cdot}69 \times 10^5$ kN/m). From equations (18) the mass of the superstructure is given as $m_s = 1130$ Mg. The value of m_s was also estimated by taking the weight of half the deck plus the weight of the top half of the piers and the calculated value which was of the order of 1000 Mg and is in agreement with the value mentioned previously.

Furthermore, Maroney *et al.* (1990) reported that, from stress–strain laboratory tests on core samples from existing bridges, the Young's modulus of the concrete was $E_c = 3800$ kip/in^2 ($2{\cdot}6 \times 10^7$ kN/m^2). This value is approximately 80% less than the value of E_c obtained from empirical expressions. Under the stronger shaking

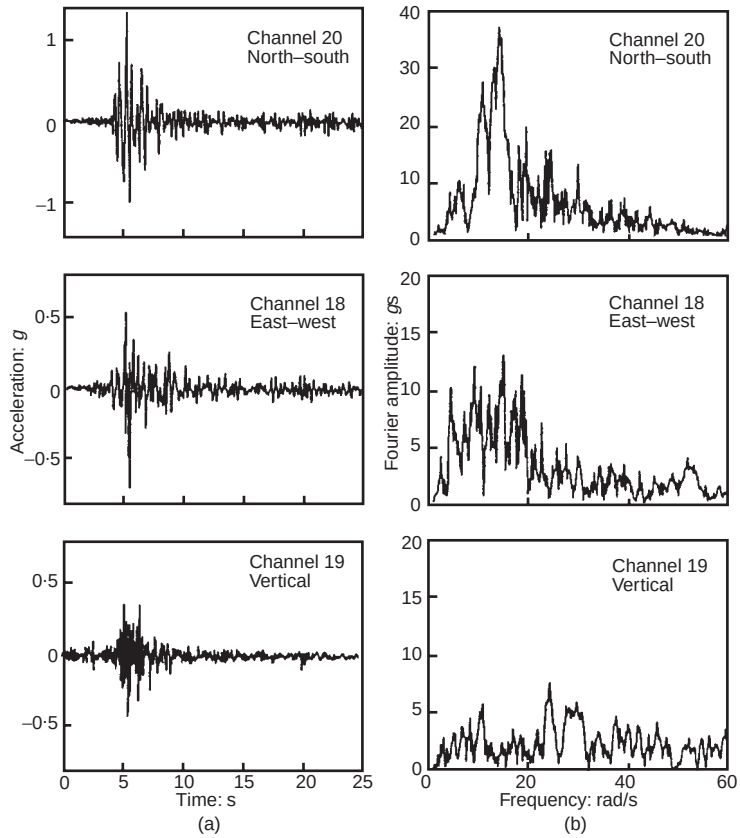

Fig. 8. Recorded time histories and Fourier amplitude spectra on the ground near the west abutment

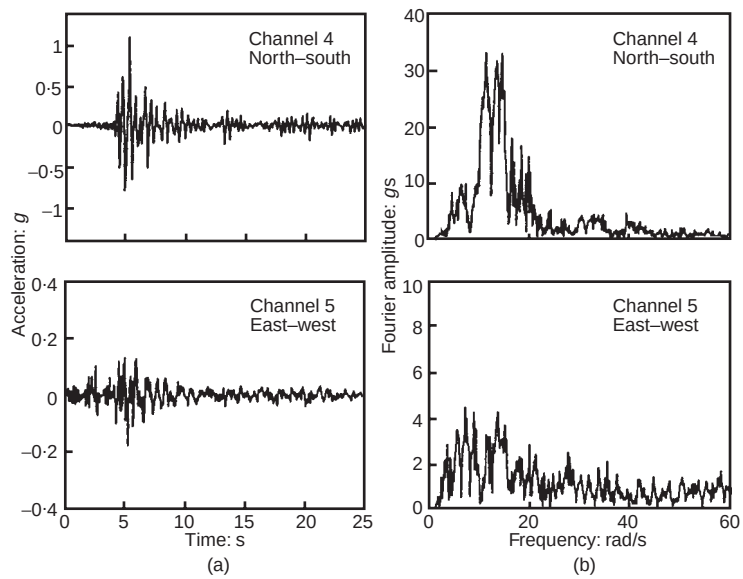

Fig. 9. Recorded time histories and Fourier amplitude spectra on the deck near the west abutment

of the Petrolia earthquake more cracking is expected to have occurred, and thus the effective value of E_c should be further reduced in an equivalent linear dynamic analysis. In this study the value of E_c reported by Maroney *et al.* (1990) is reduced by 15%. With this reduction, E_c equals 22 GPa, which is a generally accepted effective value for moderately cracked concrete. Based on this assumption, the vertical stiffness of the bridge pier K_Z^c, can be approximated by

$$K_Z^c = \frac{E_c A_c}{h_c} \approx \frac{(2{\cdot}2 \times 10^7 \text{ kN/m}^2)(1{\cdot}19 \text{ m}^2)}{6 \text{ m}} \approx 4{\cdot}4 \times 10^6 \text{ kN/m} \quad (21)$$

where A_c and h_c are the bottom cross-sectional area and the net height of the pier respectively.

The vertical stiffness of the superstructure is approximately

$$K_Z^s = 2K_Z^c \approx 8{\cdot}8 \times 10^6 \text{ kN/m} \quad (22)$$

and from equation (16)

$$\Omega_{Zs} = 96 \text{ rad/s}$$

If l is the projection to the north–south direction of the distance between the centres of the two piers ($l \approx 9{\cdot}5$ m), the rotational stiffness of the superstructure can be approximated by

$$K_R^s = \frac{K_Z^c l^2}{2} \approx \frac{(4{\cdot}4 \times 10^6 \text{ kN/m})(90 \text{ m})^2}{2} \approx 2{\cdot}0 \times 10^8 \text{ kNm/rad} \quad (23)$$

and from equation (16)

$$\Omega_{Rs} \approx 60 \text{ rad/s}$$

The moment of inertia of the deck is estimated to be $I_s \approx 20\,000$ Mgm^2 and from equation (19) the radius of gyration of the superstructure is $\rho_s = 4{\cdot}2$ m. Sensitivity studies showed that the deck response was not altered by a variation in the modulus of concrete ($20 \text{ GPa} < E_c < 26 \text{ GPa}$). Rather, the deck response is much more sensitive to the values of the foundation stiffnesses.

Soil profile and foundation parameters

Before construction, a geotechnical exploration at the location of the piers was conducted. Using standard penetration test (SPT) measurements from the ground surface down to a depth of about 10 m,

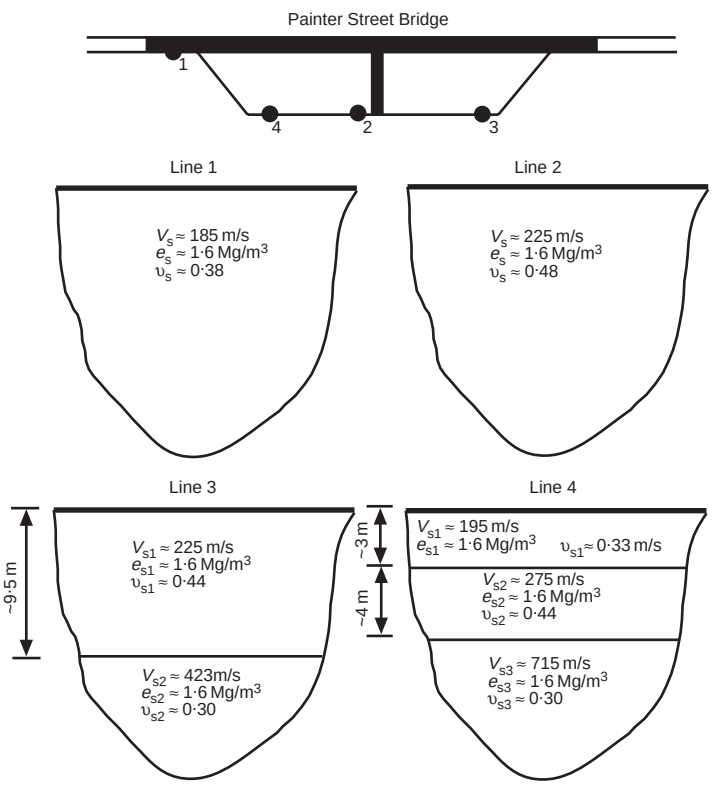

Fig. 10. Four idealized soil profiles that emerged from the refraction surveys (Heuze & Swift, 1991)

moderately stiff/dense soil layers were identified, which consisted of clayey sand, silty sand, sandy silt and gravelly sand. STP blowcounts varied from 8 near the surface to 34 at 10 m depth. The underlying stratum was a very dense gravelly and silty sand, where blowcounts exceeded 100 blows/ft.

In a geophysical exploration by Heuze & Swift (1991) six so-called seismic refraction surveys were reported, along four lines parallel to the highway. Four different idealized soil profiles have emerged as shown in Fig. 10. Evidently, the differences in the S wave velocities and shear moduli among these profiles are substantial, given that they are 20–30 m apart from each other. For instance, the resulting low-strain shear modulus from the data along line 2 has twice the value of that resulting from the data along line 1. It is quite possible that some of these differences merely reflect inadequacies (general and specific) of the seismic refraction technique. The dynamic analysis of the pile–foundation–bridge system used in this Paper is based on the values extracted from the data along line 2, which is adjacent to the pier.

Closed-form expressions for the static stiffnesses of a single pile have been derived by fitting finite element results of the static problem (Gazetas, 1984). The accuracy of these expressions has been verified by comparing their results with the solution of Blaney *et al.* (1976) for lateral and vertical pile motion in homogeneous soil, and the solution of Randolph (1981) for lateral pile motion in non-homogeneous soil with modulus proportional to depth. Using the expressions derived by Gazetas, the soil data along line 2—$G_s = 100$ MPa, $\nu_s = 0{\cdot}48$, pile diameter $d = 0{\cdot}36$ m and pile length $L = 7{\cdot}62$ m—and Young's modulus of the pile $E_p = 22\,000$ MPa, the static stiffnesses of the single fixed-head pile are approximated by

$$K_X^{[1]} \approx E_s d(E_p/E_s)^{0{\cdot}21} \approx 260 \text{ MN/m} \quad (24)$$

$$K_Z^{[1]} \approx 1{\cdot}9 G_s d(L/d)^{2/3} \approx 520 \text{ MN/m} \quad (25)$$

$$K_R^{[1]} \approx 0{\cdot}15 E_s d^3 (E_p/E_s)^{0{\cdot}75} \approx 50 \text{ MNm/rad} \quad (26)$$

$$K_{XR}^{[1]} \approx -0{\cdot}22 E_s d^2 (E_p/E_s)^{0{\cdot}5} \approx 75 \text{ MN/rad} \quad (27)$$

The horizontal $K_X^{[1]}$ and vertical $K_Z^{[1]}$ static stiffnesses of the single pile are also calculated using the procedure developed by Trochanis, Bielak & Christiano (1991) which is based on one-dimensional analysis that uses a realistic hysteretic model which has been calibrated using a three-dimensional finite element analysis of the soil–pile system. The procedure was originally developed to produce load control force–displacement curves. This procedure is modified for displacement control force–displacement curves in Fig. 11(a). The resulting horizontal static stiffness of the pile is the slope of the force–displacement curve in Fig. 11(a), which at small deflections has

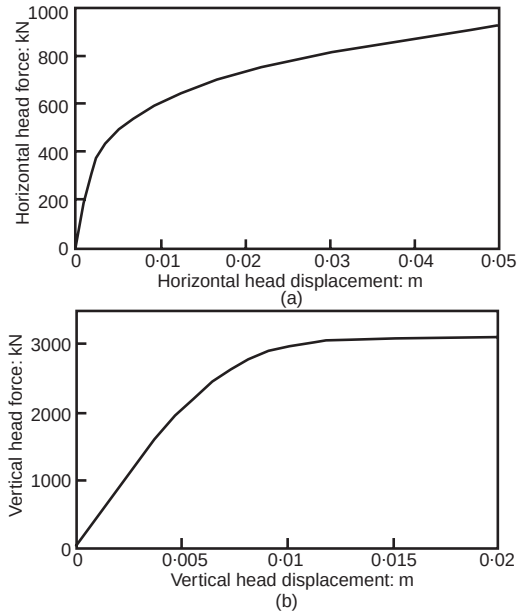

Fig. 11. Computed head force–displacement curves for single pile ($d = 0{\cdot}36$ m, $L = 7{\cdot}62$ m, $G_s = 100$ MPa, $s_u = 400$ kPa, $\nu_s = 0{\cdot}48$)

a value of approximately 200 MN/m. This value is indeed close to the value given by equation (24). The computer program developed by Trochanis *et al.* (1991) was used to produce Fig. 11(b). The initial stiffness provided by this curve is approximately 450 MN/m, which is also very close to the result of equation (25). The small amplitude vertical stiffness of the single pile is also calculated using the approximate closed-form solution derived from elasticity theory. For compressible piles in homogeneous deposits the vertical static stiffness of a single pile can be approximated by (Fleming, Wetman, Randolph & Elson, 1984)

$$K_Z^{[1]} = \frac{\dfrac{4}{1-\nu_s} + \dfrac{2\pi}{\zeta}\dfrac{\tan(\mu L)}{\mu L}\dfrac{L}{r_0}}{1 + \dfrac{1}{\pi}\dfrac{G_s}{E}\dfrac{4}{1-\nu}\dfrac{\tan(\mu L)}{\mu L}\dfrac{L}{r_0}} G_s r_0 \quad (28)$$

where ν_s is Poisson's ratio of the soil, G_s is the shear modulus of the soil, E_p is Young's modulus of the pile, L is the pile length, r_0 is the pile radius, $\zeta = \ln(L/r_0)$ and $\mu = (2G_s/E_p)^{1/2}/r_0$. For $L = 7{\cdot}62$ m, $r_0 = 0{\cdot}18$ m and $E_p/G_s \simeq 250$, equation (28) gives $K_Z^{[1]} \simeq 25 G_s r_0$. For the small-strain value $G_s = 100$ MPa, equation (28) gives $K_Z^{[1]} = 450$ MN/m, which is in good agreement with the previous results.

All the aforementioned values of pile stiffness have been calculated using the small strain value $G_s(\gamma_s < 10^{-5}) = G_{max} \simeq 100$ MPa. However, under

the Petrolia seismic excitation the level of soil strain is estimated to have been $\gamma_s \simeq 10^{-3}$ and occasionally $\gamma_s = 10^{-2}$. At this strain level the modulus of soil shear is substantially reduced and can be five times less than the small strain value G_{max} (Tatsuoka, Iwasaki, Yoshida & Fukushima, 1979). At this point average realistic values for the horizontal, vertical and cross-horizontal rocking static stiffnesses of the single pile are selected as $K_X^{[1]} = 65$ MN/m, $K_Z^{[1]} = 200$ MN/m, $K_{XR}^{[1]} = -20$ MN/rad, and the rocking stiffness of the individual piles is neglected as it is negligible compared with the rotational stiffness of the foundation system resulting from the axial vibration of piles. These stiffnesses are approximately two to four times smaller than the values obtained using the small strain value of the soil shear modulus (equations (24)–(27)). The horizontal and cross-horizontal rocking stiffnesses are reduced more than the vertical stiffness because the soil strains near the soil surface that primarily influence the horizontal pile motion are larger that the strains at greater depths on which the vertical stiffness depends.

Using the procedure described for determining the dynamic impedances, the group stiffnesses are calculated from equations (6)–(8) and (10). For instance, the horizontal and vertical dynamic stiffness coefficients for the 4×5 pile group are plotted in Fig. 12 as a function of the dimensionless frequency $a_0 = \omega d/V_s$. The normalized values of the

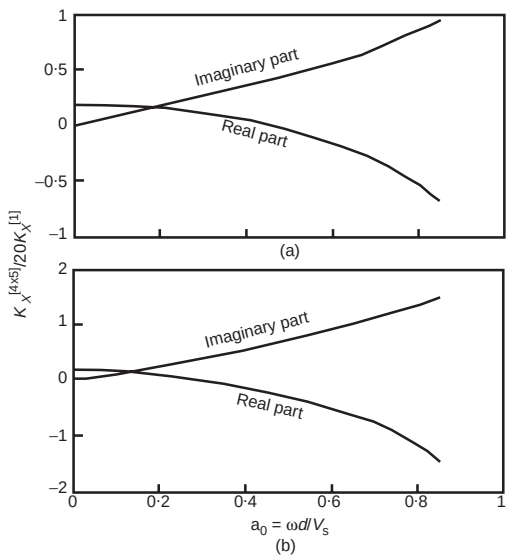

Fig. 12. Storage (real part) and loss (imaginary part) stiffness factors of a four by five pile group with rigid pile cap as a function of dimensionless frequency with $E_p/E_s = 75$, $\rho_p/\rho_s = 1{\cdot}5$, $\beta_s = 0{\cdot}05$ and $\nu_s = 0{\cdot}48$, in a homogeneous half-space: (a) horizontal motion; (b) vertical motion

real part at the zero frequency limit are 0·19 for the horizontal mode and 0·16 for the vertical mode. These values are close to 1/5, which is the value obtained by using the flexibility ratios provided in classical foundation textbooks (e.g. Fleming *et al.*, 1984). The resulting static stiffnesses for the 4×5 group are $K_X^{[4\times5]} \approx 250$ MN/m, $K_Z^{[4\times5]} \approx 600$ MN/m and $K_{XR}^{[4\times5]} \approx 300$ MN/rad.

To calculate the foundation stiffnesses of Painter Street Bridge, it is assumed that the motion of a pile in one pile group does not affect the motion of a pile belonging in the other pile-group. The minimum distance between two piles in different pile groups is $S = 8$ m, i.e. $S/d > 22$. Although for such a high value of S/d no interaction is expected between two piles, the motion of the entire pile group, which has an equivalent diameter $d_e \approx 4{\cdot}6$ m, might influence the motion of the neighbouring pile group as l/d_e is about 2·5. Nevertheless, for lack of other evidence, it is assumed that no interaction occurs. To this end, the horizontal, vertical, rocking and cross-horizontal rocking stiffnesses of the foundation of Painter Street Bridge are estimated to be

$$K_X^{[F]} \approx 2K_X^{[4\times5]} \approx 500 \text{ MN/m} \tag{29}$$

$$K_Z^{[F]} \approx 2K_Z^{[4\times5]} \approx 1200 \text{ MN/m} \tag{30}$$

$$K_R^{[F]} \approx K_Z^{[4\times5]} l^2/2 \approx 27000 \text{ MN/rad} \tag{31}$$

$$K_{XR}^{[F]} \approx 2K_{XR}^{[4\times5]} \approx 600 \text{ MN/rad} \tag{32}$$

For these and $h \approx 7$ m, equation (18) gives $\Omega_X \approx 21$ rad/s, $\Omega_Z \approx 32{\cdot}5$ rad/s, $\Omega_{Rf} \approx 22$ rad/s and $\Omega_{XRf} \approx 9$ rad/s. The mass of the foundation was estimated to be $m_f \approx 225$ Mg, and the moment of inertia $I_f \approx 8000$ Mgm^2. From equation (19) ρ_f is about 5·96 m and μ is $m_f/m_s \approx 0{\cdot}2$.

ANALYTICAL PREDICTION OF THE RESPONSE

The response of the foundation system of the bridge is calculated from equation (20) and compared against the recorded motion. Three predictions are shown. Prediction A is the result when the entire frequency dependence of the foundation impedance is considered. Prediction B is the result when the stiffness and damping of the foundation are calculated at the predominant frequency of the input motion ($f_p = 2{\cdot}32$ Hz and $\omega_p = 14{\cdot}57$ rad/s, see Fig. 6(b), channel 14). At this frequency the horizontal and vertical dynamic stiffness coefficients are $k_{X1}(14{\cdot}57) + ik_{X2}(14{\cdot}57) = 0{\cdot}970 + i0{\cdot}331$ and $k_{Z1}(14{\cdot}57) + ik_{Z2}(14{\cdot}57) = 0{\cdot}903 + i0{\cdot}545$ respectively. Prediction C is the result when the foundation is considered as a fixed, monolithic support.

Figure 13 shows the horizontal north–south motion of the pile cap of the bridge foundation. The result of prediction A agree well with the

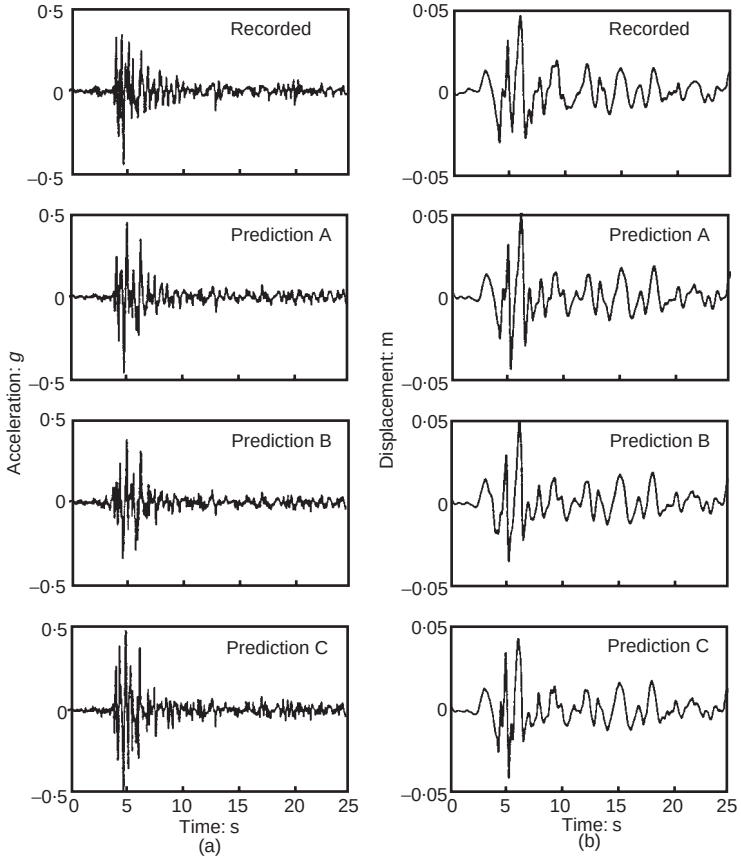

Fig. 13. Comparison of recorded north–south pile cap absolute acceleration and displacement time histories for the 1992 Petrolia earthquake seismic input (channel 3)

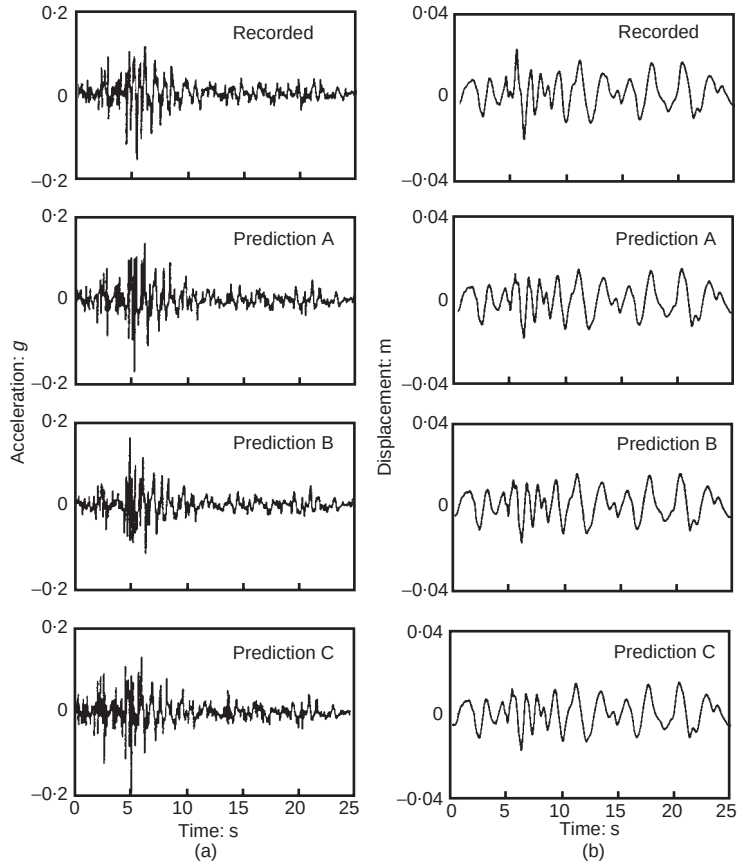

Fig. 14. Comparison of recorded vertical pile cap absolute acceleration and displacement time history for the 1992 Petrolia earthquake seismic input (channel 2)

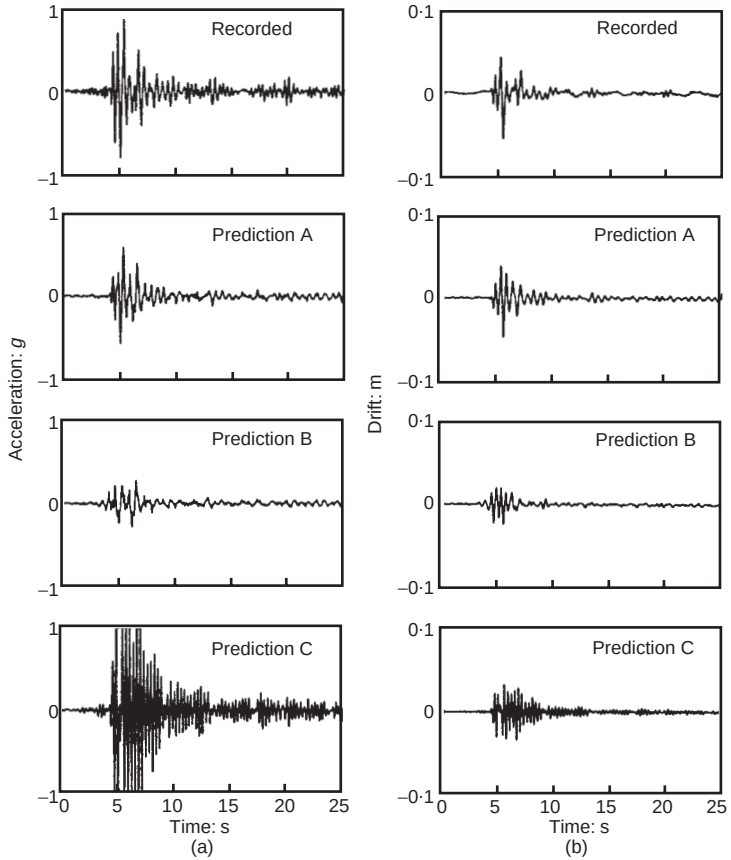

Fig. 15. Comparison of recorded north–south deck acceleration and drift time history for the 1992 Petrolia earthquake seismic input (channel 7)

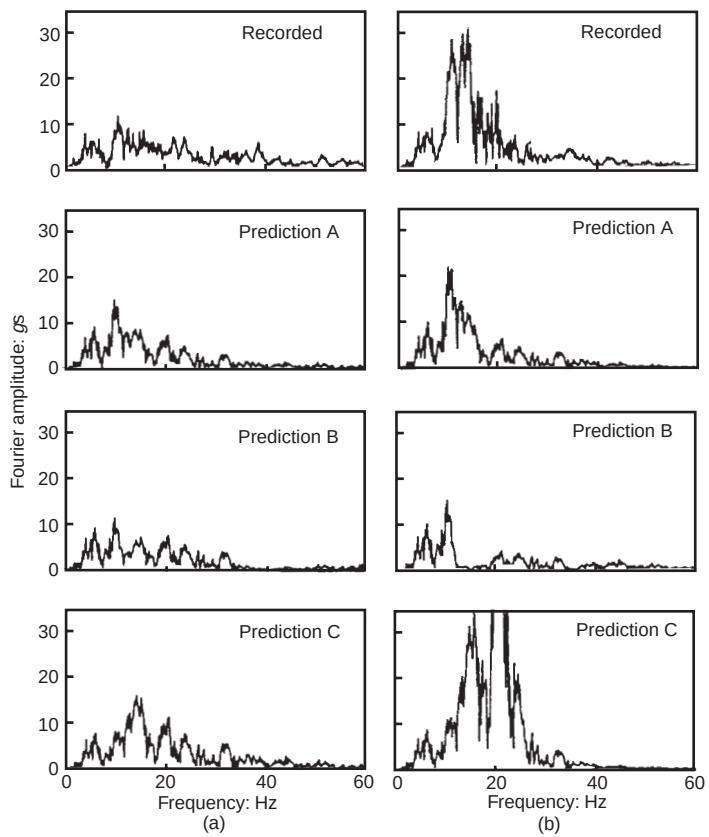

Fig. 16. Recorded and predicted Fourier amplitude spectra: (a) on the pile cap (channel 3); (b) on the deck (channel 7)

records. The peak values of both acceleration and displacement are predicted very accurately. The result for the displacement history from prediction B also agrees well with the records and the acceleration history is underestimated. Similar predictions are given from prediction C where the acceleration history is overestimated.

Figure 14 shows the vertical motion of the pile cap. Again the results of prediction A are most favourable for the peak acceleration values, whereas the total displacement histories of the three predictions are almost identical.

Figure 15 shows the horizontal north–south deck acceleration and the deck drift relative to the level of the pile cap. The results of prediction A for the deck drift are good, but the acceleration is underestimated by about 30%. There may be several reasons for this discrepancy, such as neglect of the torsional motion of the bridge about the vertical axis, yielding of the bridge pier and yielding of pile heads. Such effects are not apparent with this simple model. For instance, the deck acceleration response is very sensitive to the value of the cross-horizontal rocking stiffness of the pile foundation. As the absolute value of the cross-horizontal rocking stiffness decreases, the predicted deck acceleration becomes increasingly pronounced, reaching the recorded values when the cross-horizontal rocking stiffness is assumed to be zero. Yielding of the pile heads will reduce the value of the cross-horizontal rocking stiffness. Nevertheless if the bridge response is calculated by neglecting the moment transmitted at the pile heads the entire analysis should be redone, starting from the interaction factors given by prediction A which have to be modified for free head piles. The results offered by prediction B are less favourable, as the response is underestimated by 60%. Prediction C gives erroneous results. The acceleration of the deck is overestimated by more than 100%, and high frequencies are present.

It is a notable example where poor modelling of the foundation affects the response of the superstructure drastically. The origin of this poor prediction is the neglect of the foundation damping. By assuming a fixed, monolithic foundation no energy dissipation is allowed through the foundation (zero radiation damping), and all the induced seismic energy is trapped into the superstructure and eventually dissipated only by structural damping.

Another interesting observation is that the ratio of the deck drift to the height of the bridge pier is of the order of $\delta_r = 1\%$. Although, there is no precise value of that ratio which indicates the level of non-linearities in the structural response, structures with moderate ductility are expected to experience some non-linear behaviour when $\delta_r \simeq 1\%$.

Figure 16 plots the recorded and predicted Fourier amplitude spectra on the pile cap and on the deck. The results of prediction A are most favourable.

CONCLUSIONS

A simple integrated procedure has been presented to analyse the problem of soil–foundation–superstructure interaction using the available theories to calculate the dynamic impedances and kinematic seismic response factors of pile foundations. The procedure uses a simple structural model which can be refined easily and expanded to account for more complex structural response, such as torsional motion of the deck and input motion at the end abutments. Despite the simplicity of the model, the procedure gives encouraging results for the response of Painter Street Bridge in Rio Dell, California. The predicted response of the bridge foundation system agrees well with recorded motions. Realistic modelling of the foundation affected the prediction of the superstructural response drastically. Nevertheless, the deck acceleration response was underestimated by 30%. This suggests that, for relatively strong movement such as the Petrolia earthquake, non-linear analysis could be more realistic. However, when the structural response is non-linear, the analysis of the frequency domain used here is not valid and the response should be calculated in the time domain.

ACKNOWLEDGEMENTS

Partial financial support for this project has been provided by Shimizu Corporation, Japan, and by the Federal Highway Administration.

NOTATION

c_X	distributed damping coefficient along horizontal direction
C_X^s	damping of superstructure for motion along horizontal direction
C_Z^s	damping of superstructure for motion along vertical direction
d	pile diameter
E_c	effective Young's modulus of concrete
E_p	Young's modulus of pile
E_s	Young's modulus of soil
$F(\omega)$	excitation vector of pile–foundation superstructure system in frequency domain
G_s	shear modulus of soil
h	elevation of deck from foundation
I_f	moment of inertia of foundation
I_s	moment of inertia of superstructure
k_X	distributed spring coefficient along horizontal direction
$K_R^{[F]}$	rotational static stiffness of foundation

K_R^s rotational stiffness of superstructure
$K_X^{[F]}$ horizontal static stiffness of foundation
K_X^s horizontal stiffness of superstructure
$K_{XR}^{[F]}$ cross-horizontal-rocking static stiffness of foundation
$K_Z^{[F]}$ vertical static stiffness of foundation
K_Z^s vertical stiffness of superstructure
$\mathscr{K}_X^{[1]}$ horizontal dynamic stiffness of single pile
$\mathscr{K}_X^{[G]}$ horizontal dynamic stiffness of pile group
$\mathscr{K}_Z^{[1]}$ vertical dynamic stiffness of single pile
$\mathscr{K}_Z^{[G]}$ vertical dynamic stiffness of pile group
L pile length
m_f mass of foundation
m_s mass of superstructure
S pile-to-pile distance
$S(\omega)$ dynamic stiffness matrix of pile–foundation superstructure system
u_f horizontal displacement of foundation
u_g horizontal ground displacement
u_s horizontal displacement of superstructure
$U(\omega)$ response vector of pile–foundation superstructure system in frequency domain
v_f vertical displacement of foundation
v_g vertical ground displacement
v_s vertical displacement of superstructure
V_S shear wave velocity of soil
$\alpha(S, \theta)$ pile-to-pile interaction factor
β_s hysteretic damping of soil
θ_f rotation of foundation
ν_s Poisson's ratio of soil
ρ_f radius of gyration of foundation
ρ_s radius of gyration of superstructure
ω angular frequency

APPENDIX 1. ELEMENTS OF THE DYNAMIC STIFFNESS MATRIX [5]

$$S_{11} = -\omega^2 + 2i\omega\xi_{Xs}\Omega_{Xs} + \Omega_{Xs}^2 \tag{33}$$

$$S_{12} = S_{21} = 0 \tag{34}$$

$$S_{13} = S_{31} = \Omega_{XRs}^2 \tag{35}$$

$$S_{14} = S_{41} = -\omega^2 \tag{36}$$

$$S_{15} = S_{51} = 0 \tag{37}$$

$$S_{16} = S_{61} = -\omega^2 - \Omega_{XRs}^2 \tag{38}$$

$$S_{22} = -\omega^2 + 2i\omega\xi_{Zs}\Omega_{Zs} + \Omega_{Zs}^2 \tag{39}$$

$$S_{23} = S_{32} = S_{24} = S_{42} = 0 \tag{40}$$

$$S_{25} = S_{52} = -\omega^2 \tag{41}$$

$$S_{26} = S_{62} = 0 \tag{42}$$

$$S_{33} = -\omega^2\left(\frac{\rho_s}{h}\right) + \Omega_{Rs}^2 \tag{43}$$

$$S_{34} = S_{43} = S_{35} = S_{53} = 0 \tag{44}$$

$$S_{36} = S_{63} = -\Omega_{Rs}^2 \tag{45}$$

$$S_{44} = -\omega^2(1+\mu) + \Omega_{Xf}^2(k_{X1}^{[F]}(\omega) + ik_{X2}^{[F]}(\omega)) \tag{46}$$

$$S_{45} = S_{54} = 0 \tag{47}$$

$$S_{46} = S_{64} = -\omega^2 - \Omega_{XRf}^2(k_{XR1}^{[F]}(\omega) + ik_{XR2}^{[F]}(\omega)) \tag{48}$$

$$S_{55} = -\omega^2(1+\mu) + \Omega_{Zf}^2(k_{Z1}^{[F]}(\omega) + ik_{Z2}^{[F]}(\omega)) \tag{49}$$

$$S_{56} = S_{65} = 0 \tag{50}$$

$$S_{66} = -\omega^2(1+\mu\rho_s/h)^2 + \Omega_{Rs}^2 + \Omega_{Rf}^2(k_{R1}^{[F]}(\omega) + ik_{R2}^{[F]}(\omega)) \tag{51}$$

REFERENCES

Banerjee, P. K. & Sen, R. (1987). Dynamic behavior of axially and laterally loaded piles and pile groups. *Dynamic behavior of foundation and buried structures*, pp. 95–133. New York: Elsevier Applied Science.

Blaney, G. W., Kausel, E. & Roesset, J. M. (1976). Dynamic stiffness of piles. *Proc. 2nd Int. Conf. Numer. Meth. Geomech. Blacksburg* **2**, 1001–1012.

Clough, R. W. & Penzien, J. (1993). *Dynamics of structures*, 2nd edn. New York: McGraw-Hill.

Dobry, R. & Gazetas, G. (1988). Simple method for dynamic stiffness and damping of floating pile groups. *Géotechnique* **38**, No. 4, 557–574.

Fan, K., Gazetas, G., Kaynia, A., Kausel, E. & Ahmad, S. (1991). Kinematic seismic response of single piles and pile groups. *J. Geotech. Engng Am. Soc. Civ. Engrs* **117**, 1860–1879.

Fleming, W. G. K., Wetman, A. J., Randolph, M. F. & Elson, W. K. (1984). *Piling engineering*. Glasgow: Surrey University Press.

Gazetas, G. (1984). Seismic response of end-bearing piles. *Soil Dyn. Earthq. Engng* **3**, 82–93.

Gazetas, G. & Dobry, R. (1984a). Horizontal response of piles in layered soils. *J. Geotech. Engng Am. Soc. Civ. Engrs* **110**, 20–40.

Gazetas, G. & Dobry, R. (1984b). Single radiation damping model for piles and footings. *J. Engng Mech. Am. Soc. Civ. Engrs* **110**, 937–956.

Gazetas, G., Fan, K., Kaynia, A. & Kausel, E. (1991). Dynamic interaction factors for floating pile groups. *J. Geotech. Engng Am. Soc. Civ. Engrs* **117**, 1531–1548.

Heuze, F. E. & Swift, R. P. (1991). *Seismic refraction studies at the Painter Street Bridge site, Rio Dell, California*. Report UCRL-ID-108595. Lawrence Livermore National Laboratory.

Kavvadas, M. & Gazetas, G. (1993). Kinematic seismic response and bending of free-head piles in layered soil. *Géotechnique* **43**, No. 2, 207–222.

Kaynia, A. M. & Kausel, E. (1982). *Dynamic stiffness and seismic response of sleeved piles*. Report R80-12. Massachusetts Institute of Technology.

Kaynia, A. M. & Novak, M. (1992). Response of pile foundations to Rayleigh waves and to obliquely incident body waves. *Earthq. Engng Struct. Dyn.* **21**, 303–318.

Kuhlemeyer, R. L. (1979). Static and dynamic laterally loaded floating piles. *J. Geotech. Engng Am. Soc. Civ. Engrs* **105**, 289–304.

Makris, N. (1994). Soil–pile interaction during the passage of Rayleigh waves: an analytical solution. *Earthq. Engng Struct. Dyn.* **23**, 153–167.

Makris, N. & Badoni, D. (1995). Seismic response of pile groups under oblique-shear and Rayleigh waves. *Earthq. Engng Struct. Dyn.* **25**, 000–000.

Makris, N., Cardosa, J., Badoni, D. & Delis, E. (1993). *Soil–pile-group–superstructure interaction in applications of seismic analysis of bridges*. Report NDCE-93-001. University of Notre Dame.

Makris, N. & Gazetas, G. (1992). Dynamic pile–soil–pile interaction II: lateral and seismic response. *Earthq. Engng Struct. Dyn.* **20**, 145–162.

Makris, N. & Gazetas, G. (1993). Displacement phase differences in a harmonically oscillating pile. *Géotechnique* **43**, No. 1, 135–150.

Mamoon, S. M. & Banerjee, P. K. (1990). Response of piles and pile groups to travelling SH-waves. *Earthq. Engng Struct. Dyn.* **19**, 579–610.

Maroney, B., Romstad, K. & Chajes, M. (1990). Interpretation of Rio Dell freeway response during six recorded earthquake events. *Proc. 4th US Nat. Conf. Earthq. Engng* **1**, 1007–1016.

Novak, M. (1974). Dynamic stiffness and damping of piles. *Can. Geotech. J.* **11**, 574–598.

Novak, M. (1991). Piles under dynamic loads: State of the Art. *Proc. 2nd Int. Conf. Recent Adv. Geotech. Earthq. Engng Soil Dyn., St. Louis* **3**, 250–273.

Novak, M. & Aboul-Ella, F. (1978). Impedance functions of piles in layered media. *J. Engng Mech. Div. Am. Soc. Civ. Engrs* **104**, 643–661.

Pender, M. J. (1993). Aseismic pile foundation design analysis. *Bull. N.Z. Natn. Soc. Earthq. Engng* **26**, No. 1, 49–161.

Poulos, H. G. (1968). Analysis of the settlement of pile groups. *Géotechnique* **18**, No. 4, 449–471.

Randolph, M. F. (1977). *A theoretical study of the performance of piles*. PhD thesis, University of Cambridge.

Randolph, M. F. (1981). Response of flexible piles to lateral loading. *Géotechnique* **31**, No. 2, 247–262.

Roesset, J. M. (1984). Dynamic stiffness of pile groups. In *Pile foundations*. New York: American Society of Civil Engineers.

Roesset, J. M. & Angelides, D. (1980). Dynamic stiffness of piles. In *Numerical methods in offshore piling*, pp. 75–82. London: Institution of Civil Engineers.

Sanchez-Salinero, I. (1983). *Dynamic stiffness of pile groups: approximate solutions*. Report GR83-5. University of Texas at Austin.

Sweet, J. (1993). *A technique for nonlinear soil-structure interaction*. Report CAI-093-100. California Department of Transportation.

Tajimi, H. (1977). Seismic effects on piles, state-of-the-art report no. 2. *Proc. Int. Conf. Soil Mech.*, Specialty Session 10, 15–27.

Tatsuoka, F., Iwasaki, T., Yoshida, S. & Fukushima, S. (1979). Shear modulus and damping by drained tests on clean sand specimens reconstructed by various methods. *Soils & Fdns* **19**, 39–54.

Trochanis, A. M., Bielak, J. & Christiano, P. (1991). Simplified model for analysis of one or two piles. *J. Geotech. Engng* **117**, 448–466.

Veletsos, A. S. & Ventura, C. E. (1985). Dynamic analysis of structures by the DFT method. *J. Struct. Engng Am. Soc. Civ. Engrs* **111**, 2625–2642.